Electronic Supplementary Information

Fluoride-enhanced Lanthanide Luminescence and White-light Emitting in Multifunctional Heteropentanuclear Al_3Ln_2 (Ln = Nd, Eu, Yb) Complexes

Hai-Bing Xu,[a] Xiao-Ming Chen,[b*] Qi-Shen Zhang,[a] Li-Yi Zhang,[a] and Zhong-Ning Chen[a*]

[a] *State Key Laboratory of Structural Chemistry, Fujian Institute of Research on the Structure of Matter, the Chinese Academy of Sciences, Fuzhou, Fujian 350002, China*

[b] *MOE Key Laboratory of Bioinorganic and Synthetic Chemistry, School of Chemistry and Chemical Engineering, Sun Yat-Sen University, Guangzhou 510275, China*

Experimental Section

General procedures. All manipulations were performed under dry argon atmosphere using Schlenk technique and vacuum-line system. The solvents were dried, distilled and degassed prior to use except those for spectroscopic measurements were of spectroscopic grade. Aluminum isopropoxide, 4-hydroxybenzonitrile (HOC_6H_4CN), 2-methyl-8-hydroxyquinoline (HMq) hexafluoroacetylacetone (Hhfac) and tetra-n-butylammonium fluoride trihydrate ($[Bu_4N]F\cdot3H_2O$) were commercially available. $Ln(hfac)_3(H_2O)_2$ (Ln = Nd, Eu, Yb) were prepared by the literature procedures.[1] All of these materials were used as received without further purification except that tetra-n-butylammonium fluoride trihydrate in spectroscopic grade dichloromethane was treated with calcium hydride before used.

Synthesis of $Al(Mq)_2(OC_6H_4CN)$ (1). 2-Methyl-8-hydroxylquinoline (318 mg, 2 mmol), aluminum isopropoxide (204 mg, 1 mmol) and 4-hydroxybenzonitrile (238 mg, 2 mmol) were added to 60 mL of absolute ethanol with stirring at 85ºC for 6 h. A precipitate occured during the heating, which was isolated and recrystallized in dichloromethane-diethyl ether. Yield: 86%. Anal. Calcd for $C_{27}H_{20}AlN_3O_3$: C, 70.28; H, 4.37; N, 9.11. Found: C, 70.43; H, 4.18; N, 9.24. ESI-MS (CH_3OH–CH_2Cl_2): m/z (%) 462 (100) ($[M+H]^+$). IR (KBr, cm-1): 2218 m (C≡N). 1H NMR ($CDCl_3$, ppm): 8.05 (d, 2H, J = 8.4 Hz, Mq), 7.48 (d, 2H, J = 8.0 Hz, C_6H_4), 7.38 (t, 2H, J = 8.0 Hz, q), 7.32 (s, 2H, Mq), 7.29 (s, 2H, Mq), 7.15 (d, 4H, J = 7.6 Hz, Mq and C_6H_4), 2.94 (s, 6H, CH_3).

Synthesis of $Al_3(Mq)_4(HMq)(\mu_3\text{-}OH)_2(\mu_2\text{-}OH)_3\{Ln(hfac)_3\}_2$ (Ln = Nd 2, Eu 3, Yb 4). These Al_3Ln_2 complexes were prepared by addition of 2.1 equiv of $Ln(hfac)_3(H_2O)_2$ to 3 equiv of **1** in dichloromethane solutions with stirring for 1 h. After filtration, the concentrated dichloromethane solutions were layered with *n*-hexane to afford the products as pale yellow microcrystals which were then dried under vacuum to remove the solvant molecules.

2 (Ln = Nd). Anal. Calcd for $C_{80}H_{52}Al_3F_{36}N_5Nd_2O_{22}$: C, 38.61; H, 2.11; N, 2.81. Found: C, 38.24; H, 2.01; N, 2.70. ESI-MS (CH_3OH–CH_2Cl_2): m/z (%) 2484 $[M+H]^+$. IR (KBr, cm^{-1}): 2855m, 2929m (O–H); 1655s (C=O). Yield: 78 %.

3 (Ln = Eu). Anal. Calcd for $C_{80}H_{52}Al_3F_{36}N_5Eu_2O_{22}$: C, 38.37; H, 2.09; N, 2.80. Found: C, 37.94; H, 2.05; N, 2.74. ESI-MS (CH_3OH–CH_2Cl_2): m/z (%) 2506 $[M+H]^+$. IR (KBr, cm^{-1}): 2854m, 2930m (H–O); 1653s (C=O). Yield: 75 %.

4 (Ln = Yb). Anal. Calcd for $C_{80}H_{52}Al_3F_{36}N_5Yb_2O_{22}$: C, 37.69; H, 2.06; N, 2.75. Found: C, 37.24; H, 1.97; N, 2.69. ESI-MS (CH_3OH–CH_2Cl_2): m/z (%) 2548 $[M+H]^+$. IR (KBr, cm^{-1}): 2856m, 2933m (H–O); 1654s (C=O). Yield: 72%.

Physical Measurements. Elemental analyses (C, H, N) were carried out on a Perkin−Elmer model 240C elemental analyzer. Electrospray ion mass spectra (ESI−MS) were performed on a Finnigan LCQ mass spectrometer using dichloromethane−methanol mixture as mobile phases. UV-vis absorption spectra were measured on a Perkin–Elmer Lambda 25 UV-vis spectrophotometer. Infrared (IR) spectra were recorded on a Magna750 FT–IR spectrophotometer with KBr pellet. Emission and excitation spectra in the UV-vis region were recorded on a Perkin–Elmer LS 55 luminescence spectrometer with a red-sensitive photomultiplier type R928. Emission lifetimes in solid states and degassed solutions were determined on an Edinburgh Analytical Instrument (F900 fluorescence spectrometer) using LED laser at 397 nm excitation and the resulting emission was detected by a thermoelectrically–cooled Hamamatsu R3809 photomultiplier tube. The instrument response function at the excitation wavelength was deconvolved from the luminescence decay. Near-infrared (NIR) emission spectra were measured on an Edinburgh FLS920 fluorescence spectrometer equipped with a Hamamatsu R5509–72 supercooled photomultiplier tube at 193 K and a TM300 emission monochromator with NIR grating blazed at 1000 nm. The NIR emission spectra were corrected via a calibration curve supplied with the instrument. The emission quantum yields (Φ) of **3** in degassed dichloromethane solutions at room temperature were calculated by $\Phi_s = \Phi_r(B_r/B_s)(n_s/n_r)^2(D_s/D_r)$ using $[Ru(bpy)_3](PF_6)_2$ in acetonitrile as the standard (Φ_{em} = 0.062); while the quantum yield of **1** and the residual Al(III)-based emission of **2**–**4** were determined relative to that of Fluorescein (Φ = 0.79) in H_2O.Where the subscripts r and s denote reference standard and the sample solution, respectively; and n, D and Φ are the refractive index of the solvents, the integrated intensity and the luminescence quantum yield, respectively. The quantity B is calculated by $B = 1–10^{-AL}$, where **A** is the absorbance at the excitation wavelength and L is the optical path length.[2,3] All the solutions used for determination of emission lifetimes and quantum yields were prepared under vacuum in a 10 cm^3 round bottom flask equipped with a side arm 1 cm fluorescence cuvette and sealed from the atmosphere by a quick-release teflon stopper. Solutions used for luminescence determination were prepared after rigorous removal of oxygen by three successive freeze-pump-thaw cycles.

Crystal Structural Determination. Single crystals of **2** suitable for X-ray diffraction were grown by layering *n*-hexane onto the dichloromethane solutions. Crystals coated with epoxy resin or sealed in capillaries with mother liquors were measured on a SIEMENS SMART CCD diffractometer by ω scan technique at room temperature using graphite-monochromated Mo-Kα radiation (λ = 0.71073 Å). Lp and absorption corrections were carried out in the reflection reduction process. The structures were solved by direct method and the heavy atoms were located from E-map. The remaining non-hydrogen atoms were determined from the successive difference Fourier syntheses. The non-hydrogen and F atoms were refined anisotropically, and the hydrogen atoms were generated geometrically with isotropic thermal parameters. The structures were refined on F^2 by full-matrix least-squares methods using the SHELXTL-97 program package.[4] For **2**, the refinements were carried out by fixing the C–F distances (1.31 ± 0.01 Å) with the occupancy factors of F1–F36 and F1'–F36' being 0.5, respectively. The selected interatomic distances (Å) and bond angles (deg) are presented in Table S1. CCDC-727234 contains the supplementary crystallographic data for this paper. These data can be obtained free of charge via www.ccdc.cam.ac.uk/conts/retrieving. html (or from the Cambridge Crystallographic Data Centre,12 Union Road, Cambridge CB2 1EZ, UK; fax: (+44) 1223 336 033; or deposit@ccdc.cam.ac.uk).

Thin Film Preparation: Transparent films of Al_3Ln_2 (Ln = Eu **3**, Yb **4**) complexes were prepared by spin-coating. A dichloromethane (0.5 mL) solution of Al_3Ln_2 (10 mg) mixed with a 1,2-dichloroethane (1 mL) solution of polymethyl methacrylate (PMMA, 50 mg) were used for spin-coating (1500 rpm).

Solid sample for white-light emission: The diluted solid-state sample was prepared by immersing 1.2 g of silica gel into 5 mL of dichloromethane containing 10 mg of **3** with stirring for five minutes, where the solvent was then removed by evaporation to dryness.

Reference

1. H.-B. Xu, J. Ni, K.-J. Chen, L.-Y. Zhang, Z.-N. Chen, *Organometallics* 2008, **27**, 5665.

2. Caspar, J. V.; Meyer, T. J. *J. Am. Chem. Soc.* **1983**, *105*, 5583. (b) Demas, J. N.; Crosby, G. A. *J. Phys. Chem.* 1971, **75**, 991. (c) Chan, S. C.; Chan, M. C. W.; Wang, Y.; Che, C. M.; Cheung, K. K.; Zhu, N. *Chem. Eur. J.* 2001, **7**, 4180.

3. Umberger, J. Q.; LaMer, V. K. *J. Am. Chem. Soc.*, 1945, **67**, 1099.

4. Sheldrick, G. M. 1997, SHELXS-97 and SHELXL-97, university of Göttingen, Germany.

Table S1. Selected interatomic distances (Å) and bond angles (deg) for **2**

Al1–O1	1.871(3)	Al1–O2	1.827(3)
Al1–O9	1.908(3)	Al1–O10	1.905(3)
Al1–N1	2.081(4)	Al1–N2	2.142(4)
Al2–O3	1.839(3)	Al2–O4	1.871(3)
Al2–O5	1.912(3)	Al2–O11	1.872(3)
Al2–N3	2.176(4)	Al2–N4	2.096(4)
Al3-O5	1.958(3)	Al3–O6	1.854(3)
Al3–O7	1.841(3)	Al3–O9	1.954(3)
Al3–O10	1.935(3)	Al3–O11	1.875(3)
Nd1–O4	2.565(3)	Nd1–O5	2.589(3)
Nd1–O7	2.410(3)	Nd1–O110	2.464(3)
Nd2–O1	2.575(3)	Nd2–O6	2.440(3)
Nd2–O9	2.588(3)	O1–C8	1.354(5)
O2–C18	1.343(5)	O6–C41	1.439(7)
O2–Al1–O1	177.09(15)	O1–Al1–O10	91.53(12)
O2–Al1–O10	88.10(13)	O2–Al1–O9	93.62(13)
O1–Al1–O9	83.47(12)	O10–Al1–O9	81.21(12)
O2–Al1–N1	99.55(15)	O1–Al1–N1	83.35(14)
O10–Al1–N1	93.97(13)	O9–Al1–N1	165.84(14)
O2–Al1–N2	81.59(14)	O1–Al1–N2	98.68(14)
O10–Al1–N2	169.52(15)	O7–Al3–O11	95.09(13)
O7–Al3–O6	95.82(13)	O6–Al3–O11	96.87(13)
O7–Al3–O10	92.72(12)	O6–Al3–O10	92.83(13)
O11–Al3–O10	166.86(13)	O7–Al3–O9	172.02(13)
O6–Al3–O9	84.79(12)	O11–Al3–O9	92.73(12)
O10–Al3–O9	79.30(11)	O7–Al3–O5	85.32(12)
O6–Al3–O5	176.57(13)	O11–Al3–O5	79.80(12)
O10–Al3–O5	90.34(12)	O9–Al3–O5	94.53(11)
O108–Nd1–O7	82.08(11)	O108–Nd1–O112	136.63(11)
O7–Nd1–O112	84.87(10)	O108–Nd1–O109	86.57(13)
O7–Nd1–O109	133.75(11)	O112–Nd1–O109	73.36(11)
O108–Nd1–O110	71.51(13)	O7–Nd1–O110	144.99(11)
O112–Nd1–O110	130.14(11)	O109–Nd1–O110	68.30(11)
O108–Nd1–O111	143.96(12)	O7–Nd1–O111	132.03(10)
O112–Nd1–O111	68.38(11)	O109–Nd1–O111	76.68(13)
O110–Nd1–O111	72.68(13)	O108–Nd1–O4	86.02(11)
O7–Nd1–O4	79.64(9)	O112–Nd1–O4	131.73(9)
O109–Nd1–O4	144.12(10)	O110–Nd1–O4	76.06(10)
O111–Nd1–O4	89.24(11)	O108–Nd1–O107	67.23(11)
O7–Nd1–O107	67.73(10)	O112–Nd1–O107	69.53(11)
O109–Nd1–O107	66.53(12)	O110–Nd1–O107	119.14(11)
O111–Nd1–O107	130.08(12)	O4–Nd1–O107	139.74(11)
O108–Nd1–O5	131.72(11)	O7–Nd1–O5	61.92(8)
O112–Nd1–O5	74.16(9)	O109–Nd1–O5	141.50(11)
O110–Nd1–O5	121.60(10)	O111–Nd1–O5	72.54(10)
O4–Nd1–O5	58.16(9)	O107–Nd1–O5	119.22(9)
C8–O1–Nd2	133.8(3)	Al1–O1–C8	115.2(3)
Al1–O1–Nd2	109.88(12)	Al1–O2–C18	118.9(3)

Nd1–O4–Al2	110.64(12)	Al2–O5–Al3	96.79(13)
Nd1–O5–Al3	100.79(10)	Al3–O6–Nd2	110.90(12)
C41–O6–Nd2	128.7(3)	Al3–O7–Nd1	111.40(12)
Al3–O10–Al1	99.40(12)	Al2–O11–Al3	101.14(14)

Table S2. PL Lifetime data of **3** and **4** as solid powder samples, in solutions, and as a thin films.

Sample type and complex [a]	Lifetimes τ (μs) [b]	Emissive intensity enhancement ***I*** [c]
	powder	
3	94.9	$\boldsymbol{I}_{\mathbf{3S}}$
3-F$^-$	187.5	5.5 $\boldsymbol{I}_{\mathbf{3S}}$
4	9.9	$\boldsymbol{I}_{\mathbf{4S}}$
4-F$^-$	13.0	1.4 $\boldsymbol{I}_{\mathbf{4S}}$
	CH_2Cl_2	
3	250.8	$\boldsymbol{I}_{\mathbf{3L}}$
3-F$^-$	577	8.4 $\boldsymbol{I}_{\mathbf{3L}}$
4	13.6	$\boldsymbol{I}_{\mathbf{4L}}$
4-F$^-$	18.0	2.2 $\boldsymbol{I}_{\mathbf{4L}}$
	Film	
3	248.9	$\boldsymbol{I}_{\mathbf{3F}}$
3-F$^-$	389.7	10.4 $\boldsymbol{I}_{\mathbf{3F}}$
4	14.8	$\boldsymbol{I}_{\mathbf{4F}}$
4-F$^-$	17.2	2.5 $\boldsymbol{I}_{\mathbf{4F}}$

[a] n-F$^-$ represent sample prepared by mixing the 0.6 equiv. of F$^-$ with complex n. [b] Excitation wavelength 335 nm. [c] For clarity, the emissive intensity enhancement (***I***) of different compounds are normalized as $I(_{nS}\ /\ _{nL\ or\ nF})$, respectively.

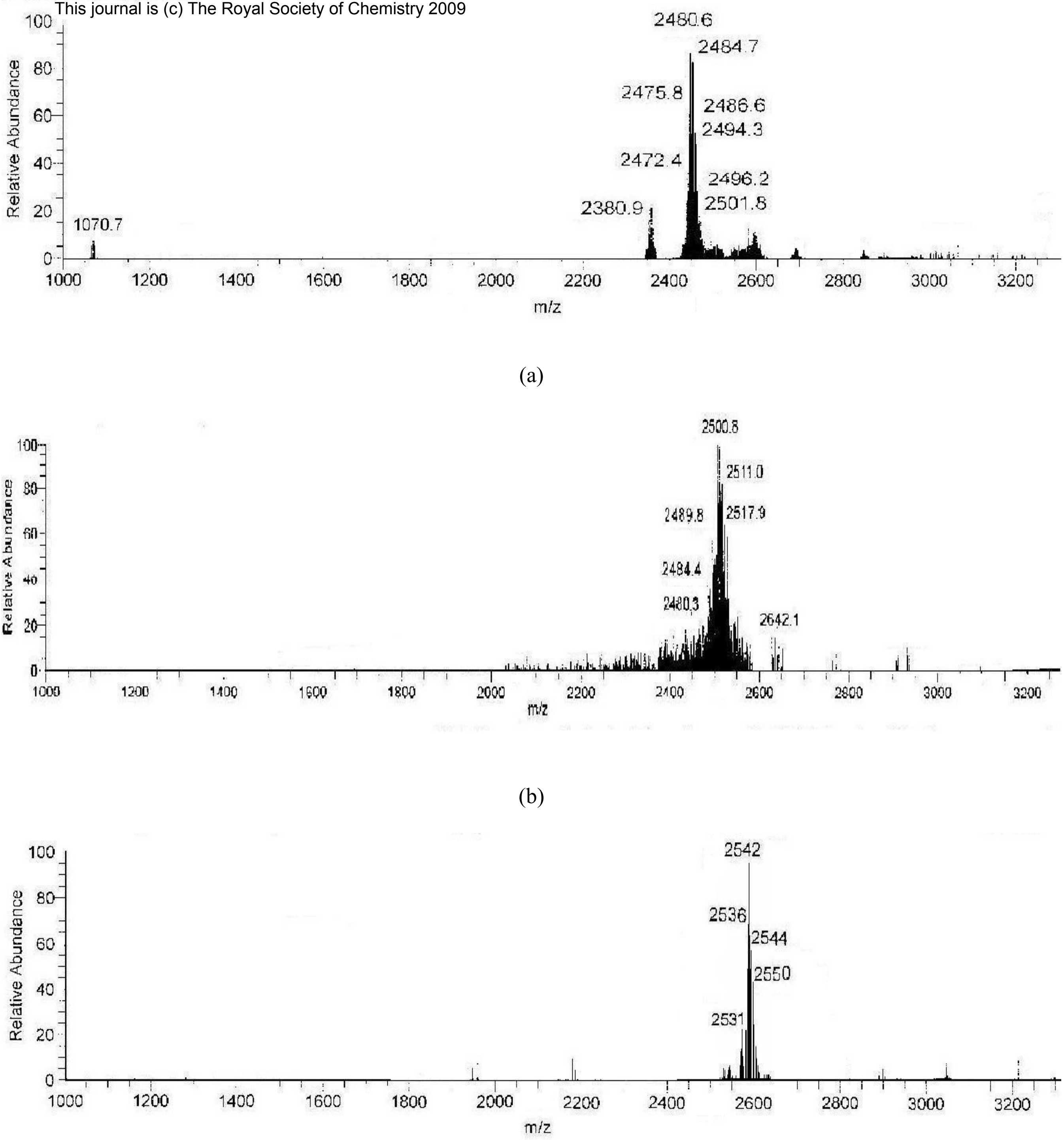

(a)

(b)

(c)

Fig. S1. ESI−MS of **2** (a), **3** (b) and **4** (c) in $CH_3OH-CH_2Cl_2$ solutions

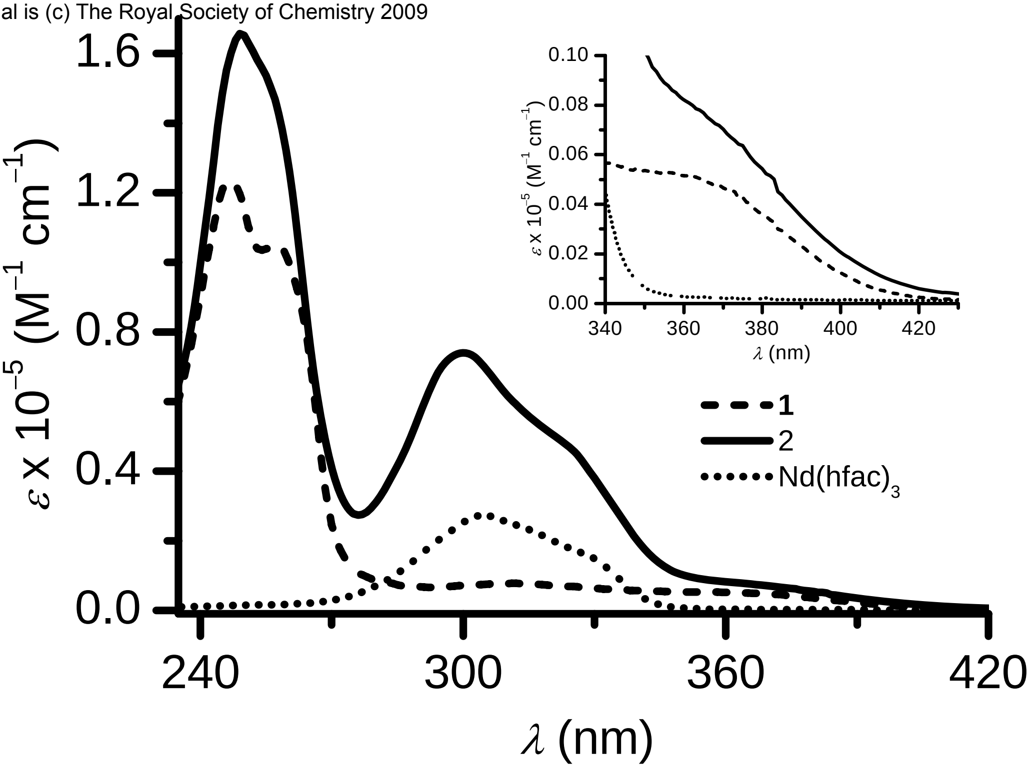

Fig. S2. The UV-vis absorption spectra of **1** (short dash), **2** (solid), and Nd(hfac)$_3$(H$_2$O)$_2$ (short dot).

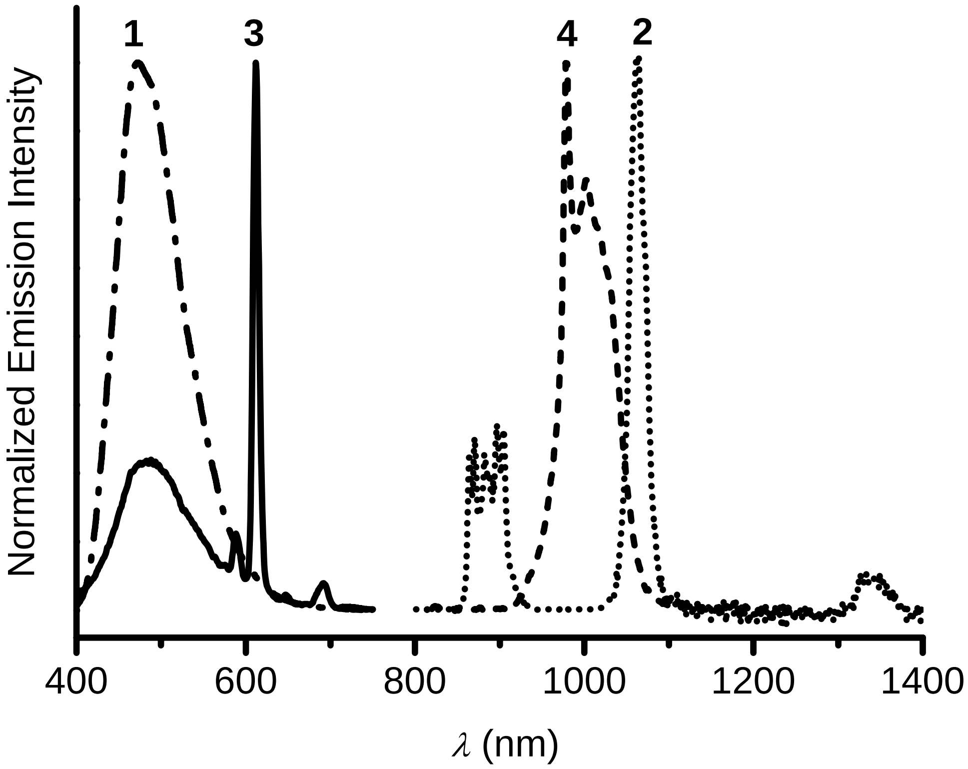

Fig. S3. Emission spectra of **1** (dash dot), **2** (short dot), **3** (solid), and **4** (short dash) in dichloromethane at ambient temperature.

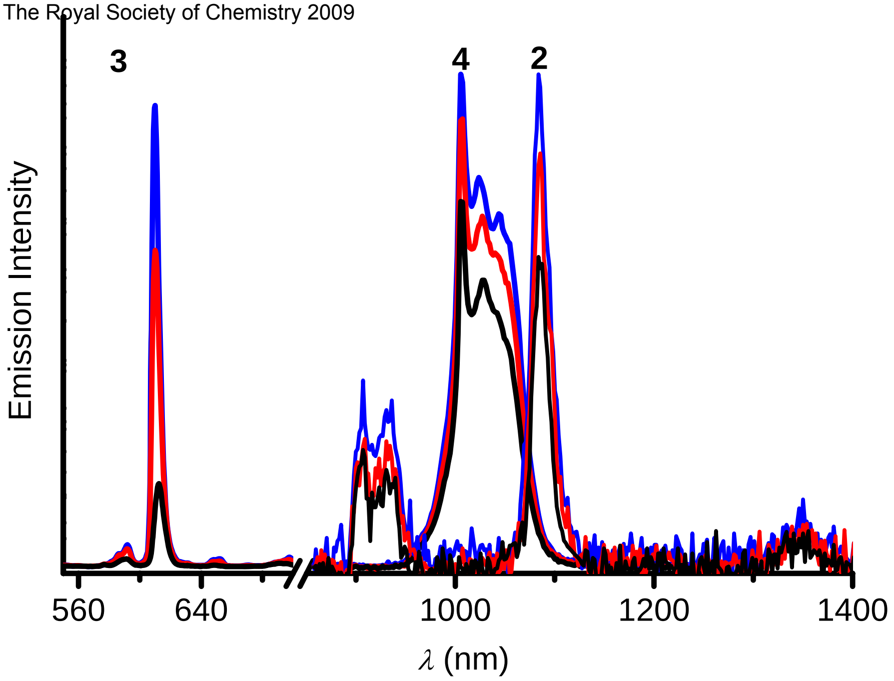

Fig. S4. Fluoride-induced lanthanide emission enhancement in dichloromethane for **2**–**4** before (black) and after addition of 0.4 (red) and 0.6 (blue) equiv of [Bu$_4$N]F at ambient temperature.

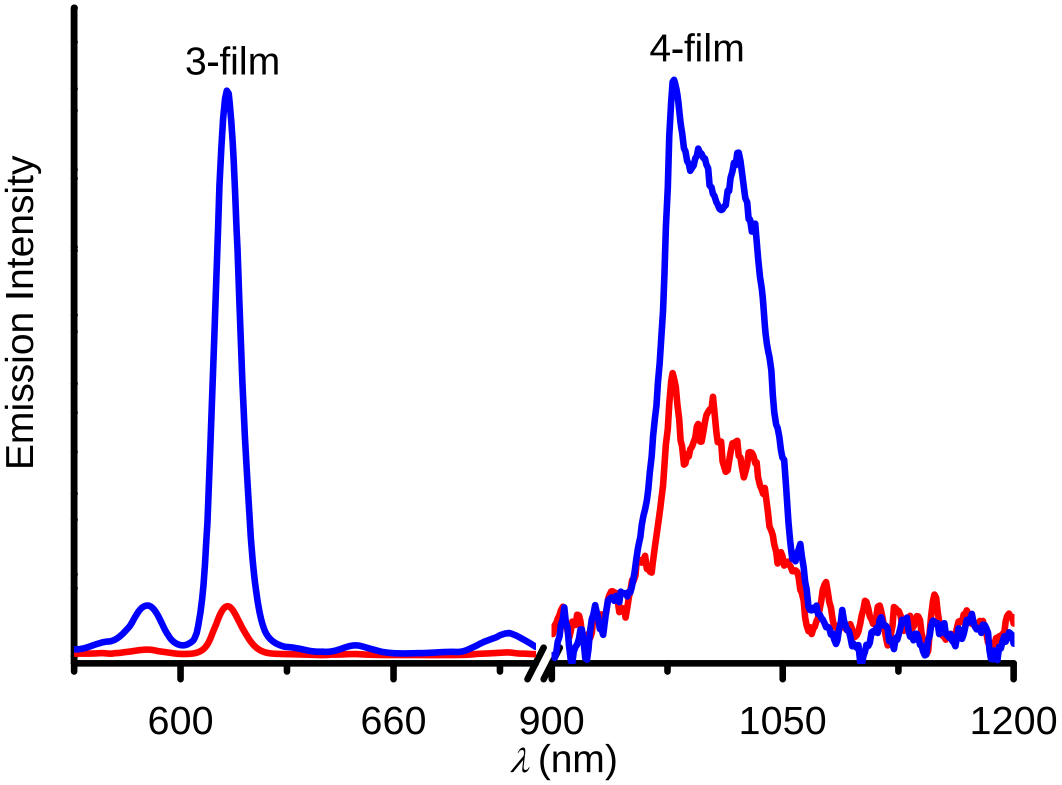

Fig. S5. Fluoride-induced lanthanide emission enhancement in thin film of PMMA for **3**–**4** before (red) and after addition of 0.6 equiv of [Bu$_4$N]F (blue) at ambient temperature.

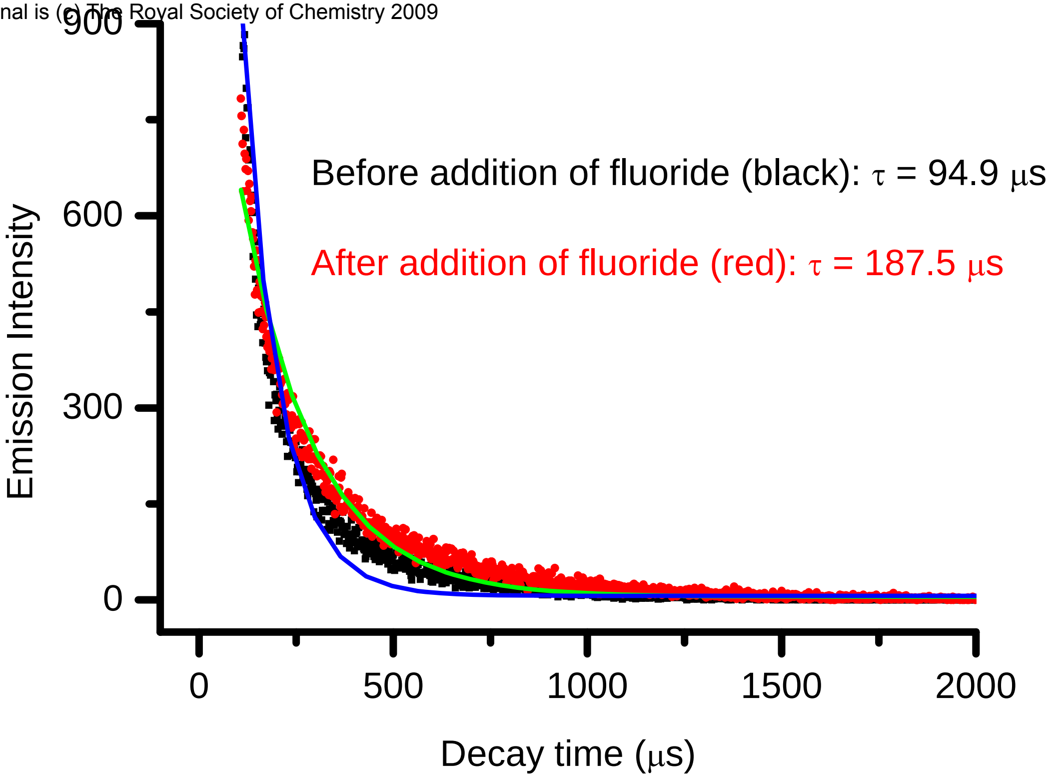

(a) **3** (solid)

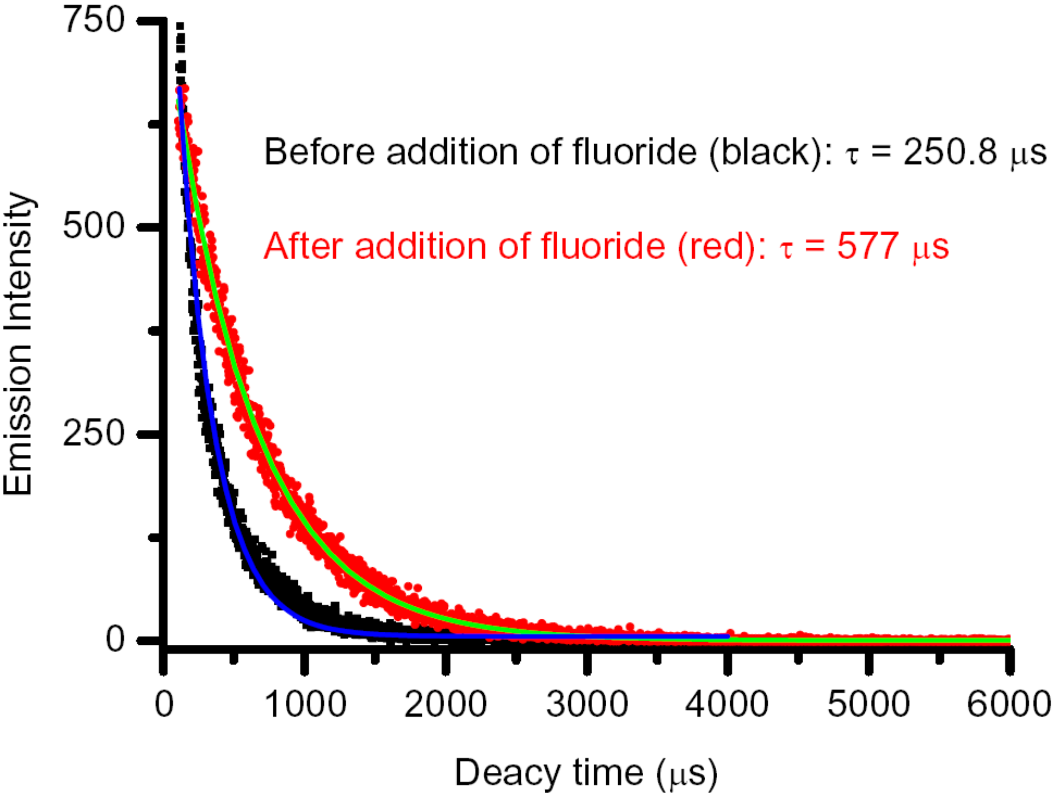

(b) **3** (CH_2Cl_2)

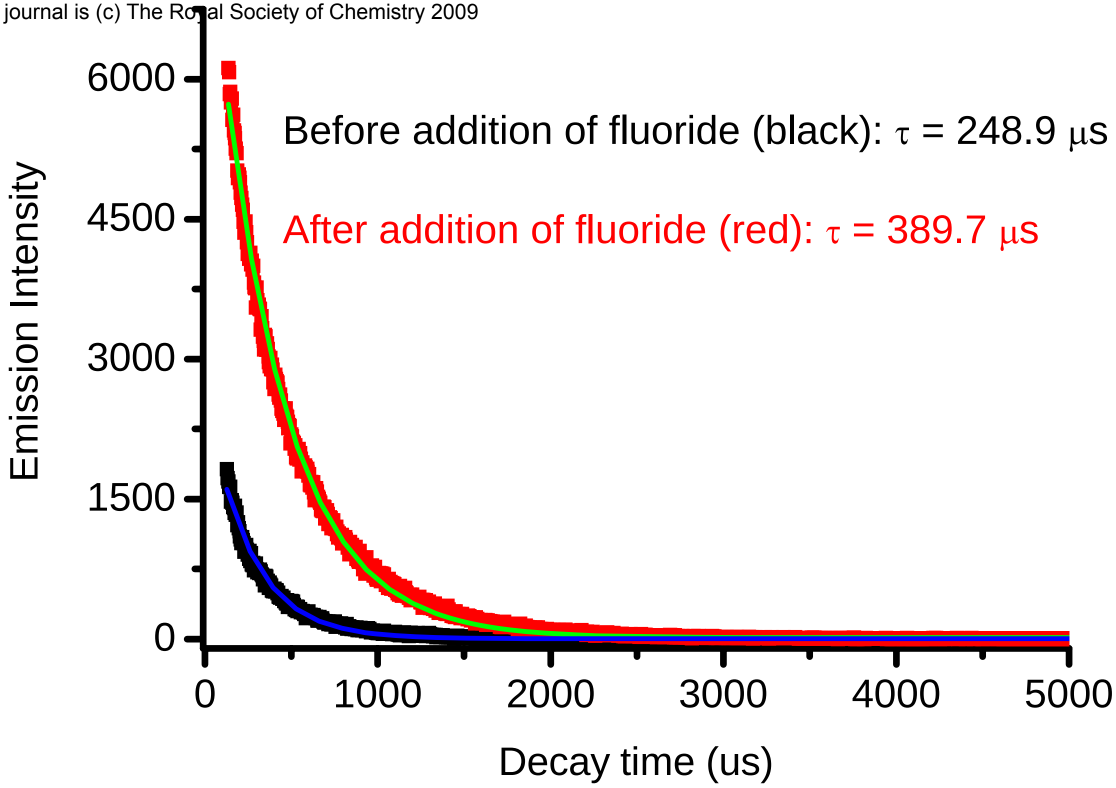

(c) **3** (film)

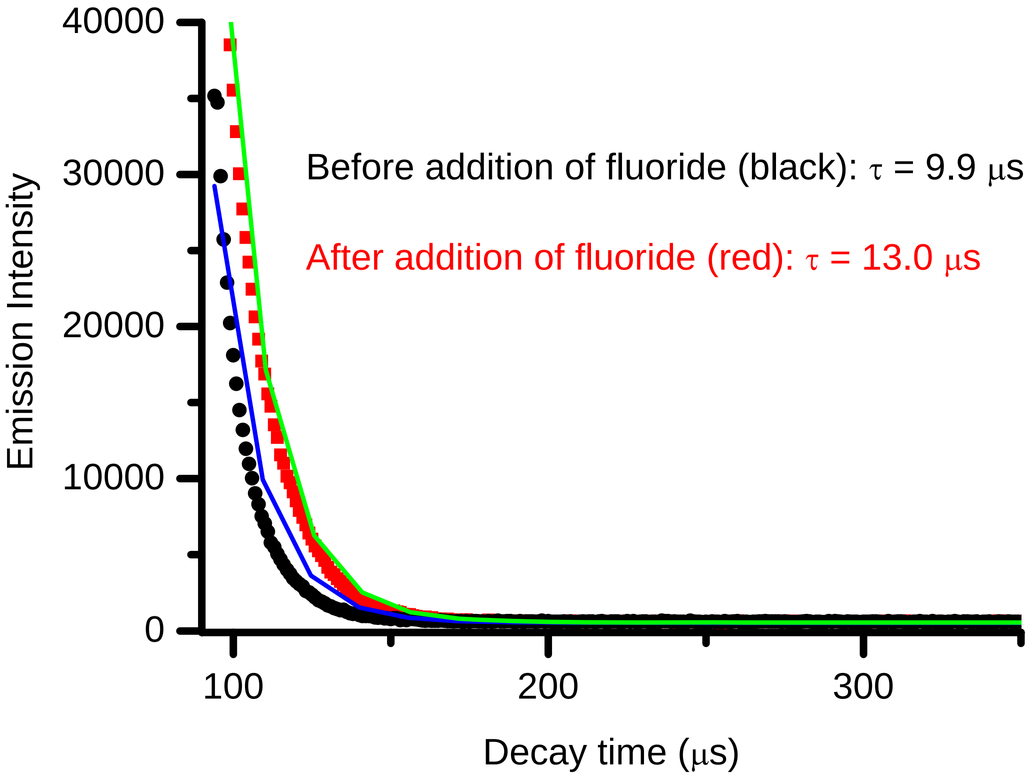

(d) **4** (solid)

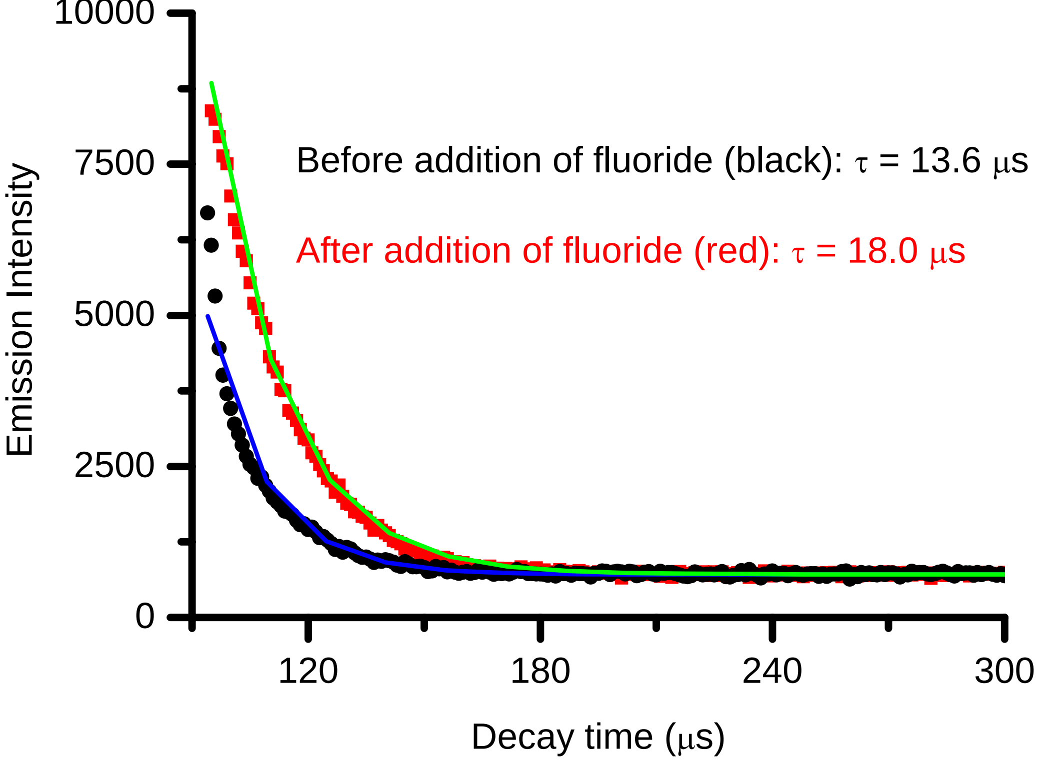

(e) **4** (CH_2Cl_2)

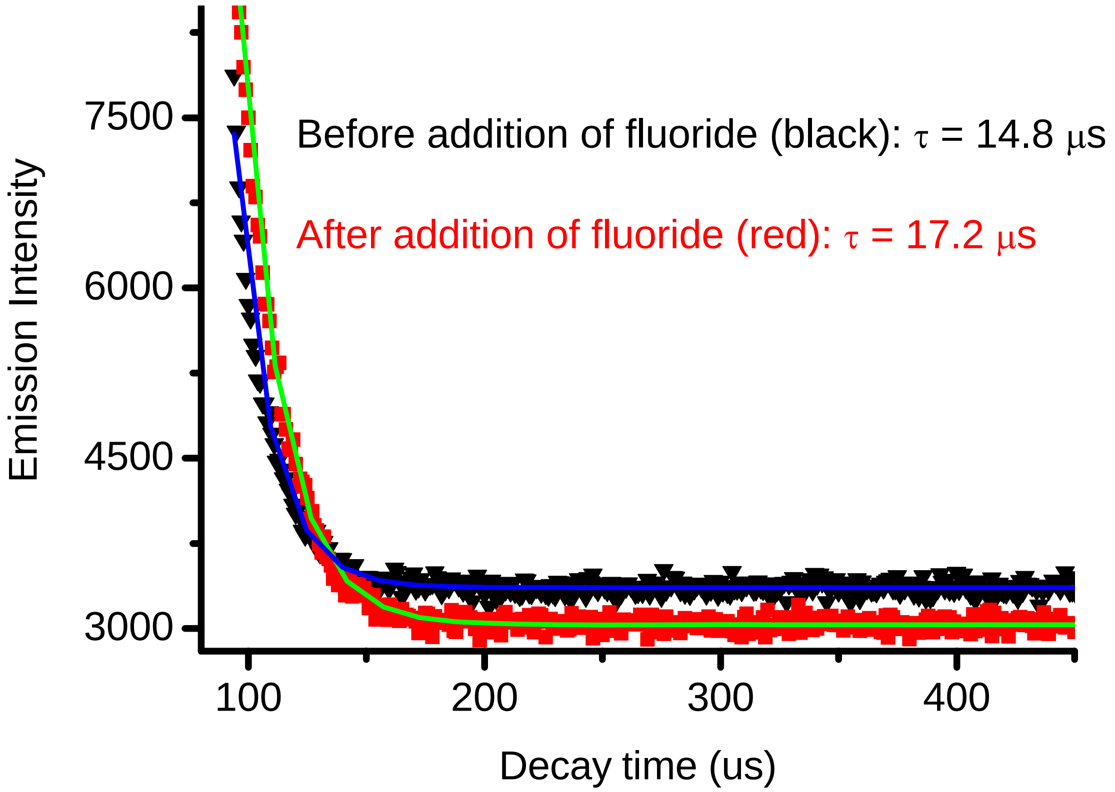

(f) **4**-film

Fig. S6. Comparison of the changes of lifetime decay curves of **3** and **4** before (black) and after (red) addition of $[Bu_4N]F$ (the molar ratio of fluoride to **3** and **4** are 0.6 : 1, respectively).

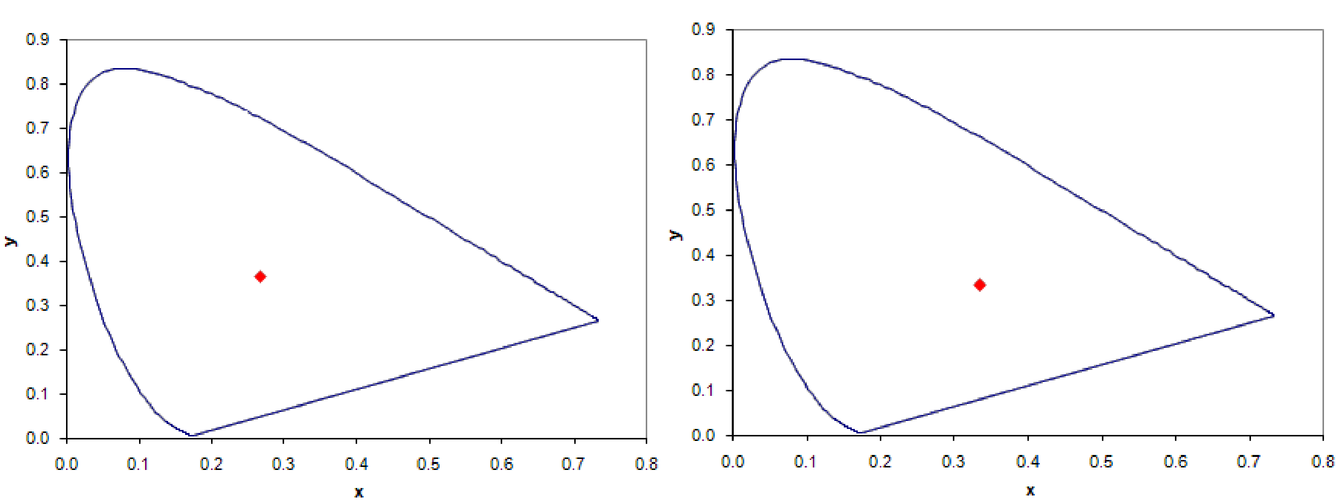

(a)

(b)

Fig. S7. The changes of chromaticity coordinates of **3** according to the International Commission on Illumination (CIE) 1931 color space chromaticity diagram without (a) and addition of 0.6 equiv. of fluoride (b).

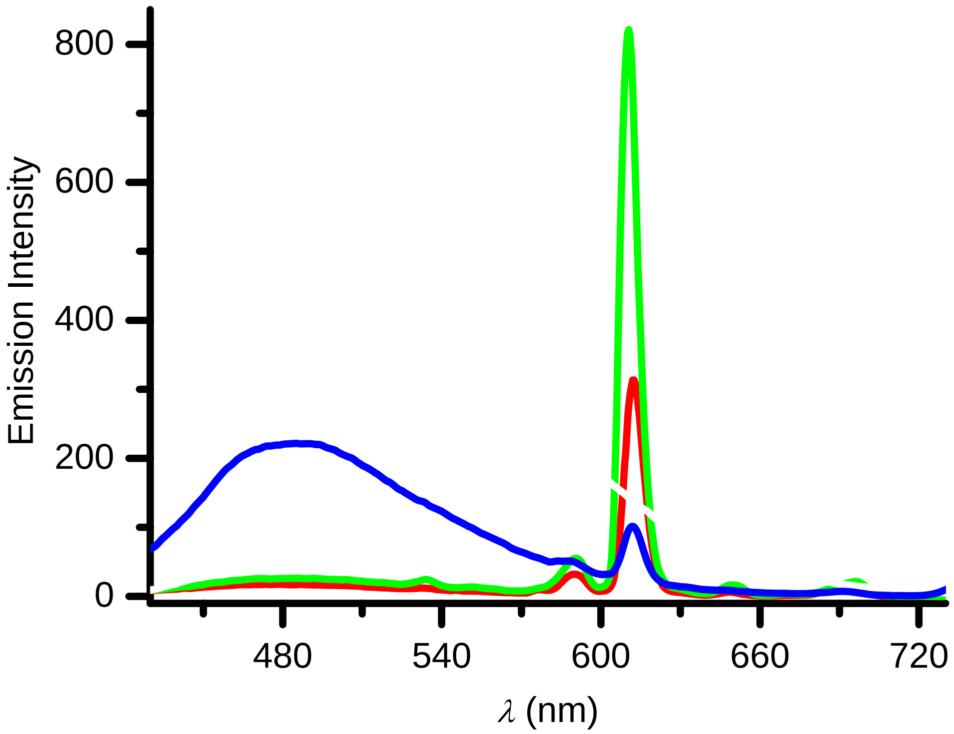

Fig. S8. Emission spectra of **3** in dichloromethane before (red) and after addition of 0.6 (green) and 1.6 (blue) equiv of [Bu$_4$N]F at ambient temperature.

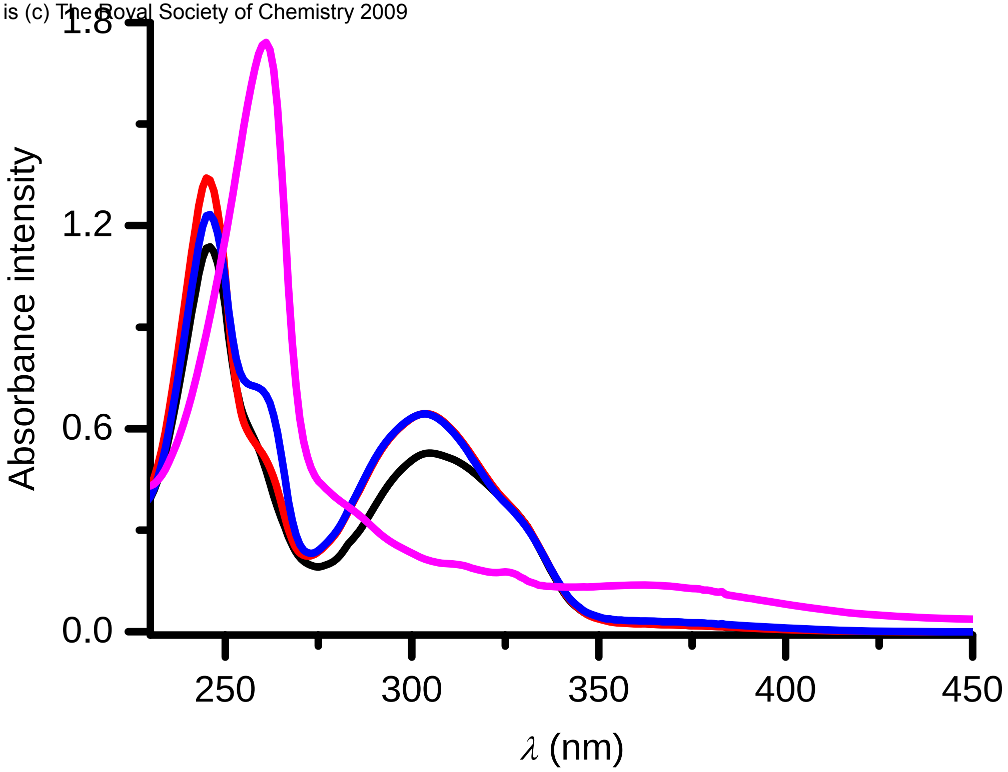

Fig. S9. UV-vis spectra in CH_2Cl_2 for **3** before (black) and after addition of 0.4 (red), 0.6 (blue) and 2 (magenta) equiv of $[Bu_4N]F$ at ambient temperature.

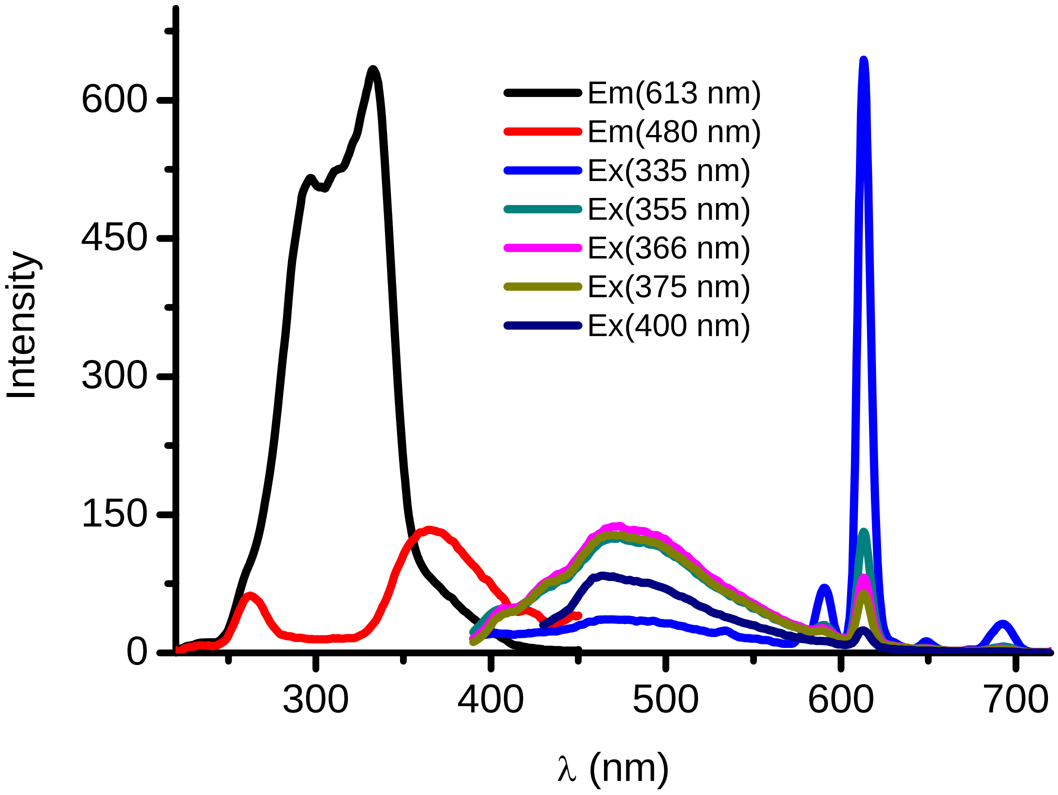

Fig. S10. Emission and excitation spectra of **3** in dichloromethane at ambient temperature.

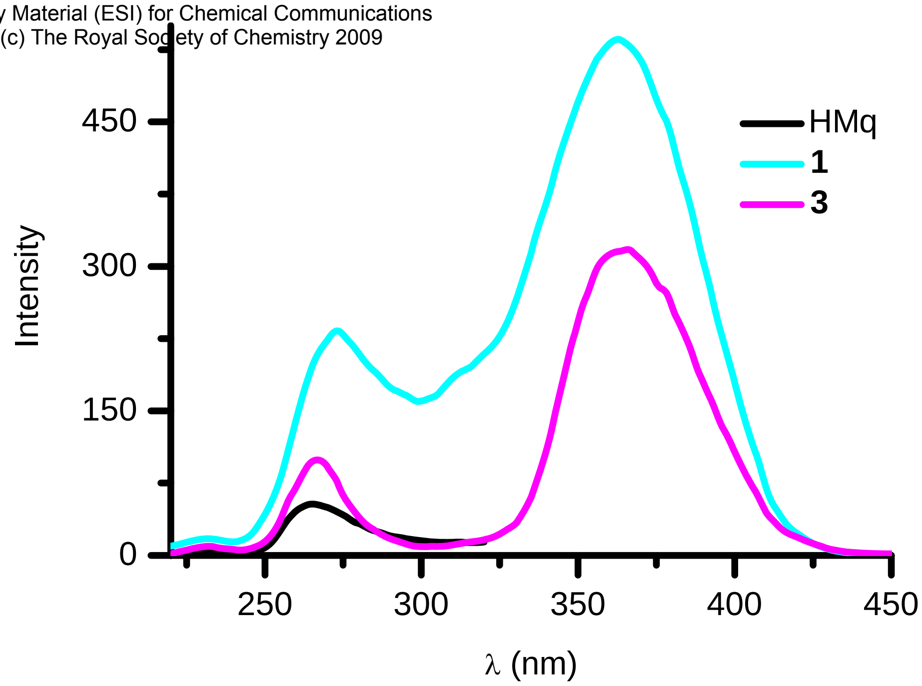

Fig. S11. Excitation spectra of **HMq**, **1** and **3** in dichloromethane at ambient temperature.